REAL TIME PROCESS CONTROL VIA IN SITU X-RAY ANALYSIS

David Palaith[a], Larry Fehrenbacher[a], Chris Deaton[b], David Wertz[c]

[a]*Technology Assessment & Transfer*
[b]*Omni Instruments*
[c]*University of Southern Mississippi*

Abstract: Intelligent control of magnetron sputtered of thin films requires in situ sensors that can interrogate the film in near real time. The incorporation of x-ray diffraction and x-ray fluorescence spectroscopy systems into an existing magnetron sputtering system at AFRL is discussed. It is shown that crystal phase, residual stress, thickness, and stoichiometry of sputtered films can be measured, and used to optimize and control the sputtering process. The potential of converting XRD and XRF data to image maps to monolor spatial uniformity of growing films is also discussed. *Copyright © 2000 IFAC*

Keywords: Image sensors, process control, sensors

1. INTRODUCTION

Development of new thin films by magnetron sputtering could benefit from intelligent process controls by reducing research and development times, shortening time-to-market, encouraging rapid response to the demand for films and coatings with tailored properties, and enabling rapid development of processing protocols for manufacturing To realize these goals, in situ sensors are necessary that can interrogate the thin film during deposition and modify processing conditions as needed and on the fly. This paper investigates the possibilities of using an in situ x-ray sensor suite to provide near real time microstructural data on thin films during sputtering.

2. MAGNETRON SPUTTERING

A magnetron is one of a class of cold cathode discharge devices in which a plasma is initiated by application of a dc or rf high voltage. The plasma is sustained by ionization caused by secondary electrons emitted from the cathode as a result of ion bombardment (Chapman, 1980). Neutral atoms, such as Ar, Ne, Kr, or Xe, are introduced into this plasma. These atoms are ionized by the plasma, after which they collide with and ablate neutral atoms from a target of the desired thin film material. These ablated atoms diffuse through the plasma and condense onto a substrate. This complicated process can be thought of as occurring in two stages: production of neutral atoms sputtered from the target (Rossnagel, 1989); film nucleation and growth on the substrate resulting in films with specific characteristics (Windishmann, 1992).

Controllable magnetron sputtering parameters include: target voltage, target current, substrate bias voltage (Haghiri-Gosnet, *et al.*, 1989), substrate temperature, substrate rotation rate, target-to-substrate distance, working gas pressure (Hoffman, *et al.*, 1990), working gas flow rate, reactive gas pressure, and reactive gas flow rate. By varying these parameter values, microscopic film properties can be altered. These properties include: crystal phases, texture, grain size, morphology stoichiometry, and residual stress (Thornton, 1974).

There are numerous methods that can be used to characterize film properties including: TEM, SEM, XPS, metallographic microscopy, and x-rays. Not all are suitable for in situ use; but x-ray analysis can be used in near real time to control the sputtering process. Two x-ray techniques are considered here: x-ray diffraction spectroscopy (XRD), and x-ray fluorescence spectroscopy (XRF). Not only can these two techniques be used to control the sputtering process, but they can be used to map the spatial uniformity of the film.

3. X-RAY DIFFRACTION SPECTROSCOPY (XRD)

XRD is one of the major standard laboratory method for investigating crystalline solids. X-rays with wavelengths $\lambda < 100$ nm are reflected from planes formed by the ordered arrangement of atoms in the solid film. Strong diffraction intensities occur when the Bragg condition

$$n\lambda = 2\,d\,\sin\Theta \qquad (1)$$

is satisfied. This condition is shown in Figure I.

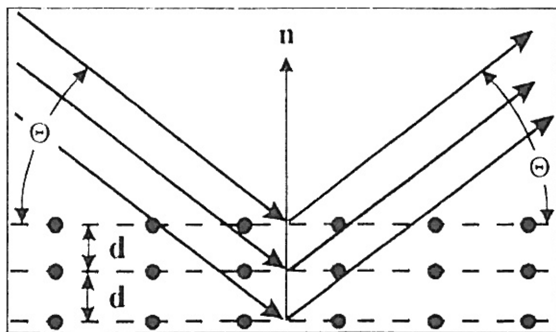

Fig. I. Diffraction of x-rays by a crystallographic plane of atoms

The diffraction order, n in Equation 1, is the number of whole wavelengths that fit within the path difference between adjacent reflection planes. Any plane through the crystal that contains a periodic array of atoms or molecules is a plane of reflection for x-rays. Thus, in general, there are many planes for which the Bragg condition will be satisfied for some incident angle.

If the material is amorphous, the atoms are not ordered into planes and the Bragg condition is never satisfied; scattering from individual atoms gives rise to a single broad maximum in the x-ray spectrum. Analysis of this curve yields such information as average inter-atomic distances, and average number of atoms around a given atom (Guinier, 1963; Warren, 1969). Frequently, crystalline and amorphous phases are mixed, or else an amorphous phase is sputtered onto a crystalline substrate. In those cases, a discrete XRD spectrum is superimposed on the broad background produced by the amorphous phase.

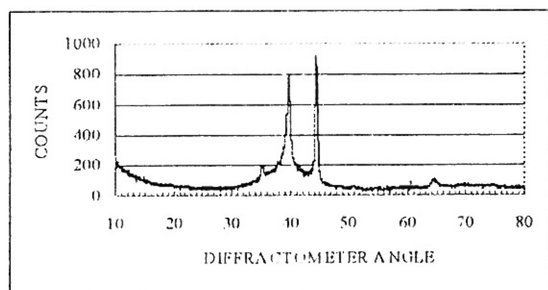

Fig. II XRD spectrum of a sputtered WS_2 thin film (film provided by AFRL)

When a thin film is deposited onto a substrate, the film goes down in a polycrystalline form, i.e. a distribution, although not necessarily random, of small crystallites. Although the film is not a single crystal, there is a high probability that Bragg's condition will be satisfied by some of these crystallites at some angle of incidence. Analysis of XRD spectra like that shown in Figure II provides complimentary microstructural information, such as residual stress and texture, in addition to crystalline phase content. It is this fact that makes it possible to use XRD to interrogate and to acquire microstructural data that can be used for controlling deposition of thin films.

4. X-RAY FLUORESCENCE SPECTROSCOPY (XRF)

X-rays also can be used to obtain the elemental stoichiometry of a thin film. When x-rays strike the atoms comprising the thin film, deep electrons in those atoms are excited to higher energy levels. When those electrons return to their ground states, they emit x-rays at energies (wavelengths) characteristic of their energy level distributions. The energy of these emitted x-rays are, therefore, characteristic of the atom that produced them. The relative intensities of these x-rays are proportional to the relative species concentration so that the spectrum of all x-ray energies can be used to determine relative elemental species concentrations, or by using calibrated standards, to determine absolute elemental species concentrations. Whereas the XRD process diffracts x-rays in specific directions, secondary XRF x-rays are emitted isotropically so that a detector does not have to be specially positioned relative to the position of the x-ray source.

In addition to obtaining stoichiometric and/or elemental species concentration, XRF also can be used to obtain film thickness. A baseline XRF spectrum of the bare substrate must be taken prior to deposition. As the film grows, the intensity of the substrate spectrum decreases due to attenuation of the secondary x-rays by the growing film, and the incnsity of the XRF spectrum characteristic of the film increases. These intensity changes are proportional to film thickness.

5. IN SITU X-RAY SENSOR SYSTEM

To apply these ideas to a real system, a XRD-XRF system was developed and retrofitted to a magnetron sputtering system at the Air Force Research Laboratory (AFRL). The sputtering chamber is shown in Figure III. It is 22 inches in diameter and contains 39 viewing ports, a vertically mounted magnetron, a sample carousel, facilities for simultaneous pulsed laser deposition, a CCD camera port, ion gauge, pump port, and manual access to the interior. These severe space restrictions required development of a unique in situ x-ray sensor system design, using only commercially available x-ray components.

The geometrical restrictions imposed by the AFRL sputtering chamber necessitated fabrication of a x-ray system simulator to evaluate each of the design concepts. The in situ simulator was used to obtain a XRD spectrum of the WS_2, and compared with the

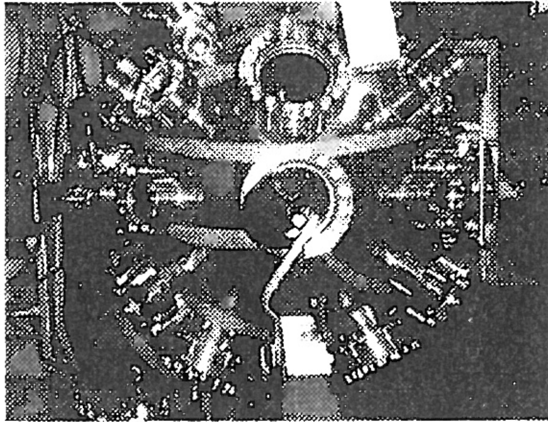

Fig. III. Magnetron sputtering chamber at AFRL

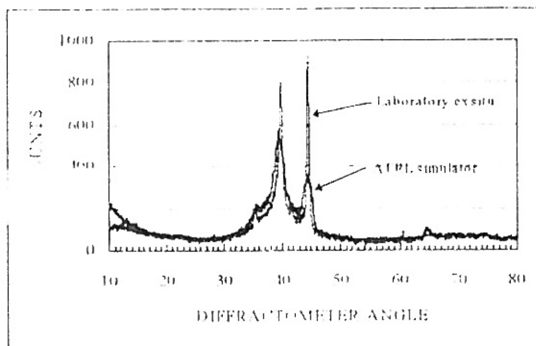

Fig. IV. XRD spectrum WS_2 thin film using AFRL in situ XRD simulator

laboratory XRD spectrum from the same film (Figure IV).

Note that the main diffraction peaks fall at the same angle Θ, confirming that the film is polycrystalline. Note also that the spectra obtained by the two different configurations exhibit different peak heights and intensities. We have demonstrated that these intensity differences can be resolved by some relatively simple preprocessing of the two spectra. In the case of XRF, no similar correction to the XRF spectrum is necessary since the secondary x-rays produced radiate isotropically.

Since the in situ x-ray system will be used for near real time process control, it is important to know the acquisition time for a XRD spectrum of interest. This can be estimated for the AFRL system from the parameters used to acquire the spectra of Figure IV. In the simulator case, a 130 mm^2 aperture was used with 0.02° and 2 s counting time per step. Such fine resolution may not be necessary for process control. For example, the useful part of the spectrum shown in Figure IV might be obtained with 0.5° steps from 33 - 50° Under these conditions, a XRD spectrum with the same signal-to-noise as that of Figure IV could be obtained in $[(50 - 33)/0.5] \times 2 = 68$ s. Thus, the larger 130 mm^2 aperture allows x-rays to interrogate a large area of the film. Therefore, this spectrum represents the average phase content of the entire film. This may be adequate for most processing conditions. But for films that require exceptional spatial uniformity, smaller apertures are necessary. Therefore, it is important to estimate the effect of aperture size on XRD and XRF spectra.

6. SPATIAL RESOLUTION

Spatial resolution ultimately will depend on the specific XRD-XRF system, and will include the effects of spurious x-ray scattering, random electronic instrument noise, detector quantum effects, and substrate and film properties. However, a general estimate of the minimum area of illumination can be made. In this discussion, the spatial resolution of XRD and XRF are treated separately.

6.1. Spatial Resolution Of the XRD Spectrum

In this discussion, the term 'noise' is used to denote any effects that introduce uncertainty into the XRD spectrum. These effects are dominated by three sources: 1. electronic noise, 2. spurious x-ray scattering – non-specular reflections – that can arise from both scattering off of the deposition chamber and x-ray hardware, and non-Bragg angle reflections off of the substrate and film itself, and 3. quantum fluctuation in the detector. At relatively large detector angles, most of the spurious x-rays should arise from x-rays scattered by the substrate, so that we may consider the substrate to be the source of all specular *and* non-specular reflections intercepted by the detector.

The total count noise, CN_T, measured as the rms number of false counts recorded, is

$$CN_T = [(CN_E)^2 + (CN_X + \sqrt{CN_X})^2 + S]^{1/2} \quad (2)$$

where CN_E is the Gaussian (also known as Johnson or Nyquist) plus 1/f count errors produced by electronic noise (Robinson, 1962), CN_X is the error in the number of x-ray photons intercepted by the detector due to spurious x-ray scattering, and S is signal level, in counts, due to x-ray diffraction at a Bragg angle. The term $\sqrt{CN_X}$ in Equation 2 arises from quantum fluctuations produced in the detector by the scattered x-rays, i.e., x-ray photons that reach the detector via non-Bragg reflections. These photons will, by themselves produce a counting error. But, in addition, there is an error in counting them, and these quantum fluctuations are equal to the square root of the count. In a similar way, the x-ray diffraction signal itself introduces an additional counting error that also is equal to the square root of the count. These quantum fluctuations are not, strictly, noise since they are caused by the signal and do not, therefore, constitute a background noise. It may be better to think of this 'noise' as a

measurement uncertainty. Consequently, this noise contribution on top of a diffraction peak is greater than the noise in the shoulders of a peak. Since CN_E, CN_X, and S are uncorrelated, their noise powers are additive as reflected in Equation 2.

The size of the aperture enters in the following way. If we have a XRD spectrum that has been acquired from an area of illumination A_o, and the peak amplitude and scattering noise are S_o and CN_{Xo} respectively, then we expect the peak amplitude and scattering noise acquired with a different area of illumination, A, to be scaled by A/A_o. Therefore, with an illumination area A, Equation 2 becomes

$$CN_T = \{|CN_E|^2 + |(A/A_o)CN_{Xo} + \sqrt{(A/A_o)}CN_{Xo}|^2 + (A/A_o)S_o\}^{1/2} \quad (3).$$

The validity of this dependence on aperture size was confirmed by ex situ laboratory measurements using a conventional x-ray diffractometer. Electronic instrument noise contributed a random error of 2.7 counts.

The signal-to-noise *at a diffraction peak* is then

$$S/N = \frac{\frac{A}{A_o} S_o}{\sqrt{(CN_E)^2 + \left(\frac{A}{A_o} CN_{Xo} + \sqrt{\frac{A}{A_o}} CN_{Xo}\right)^2 + \frac{A}{A_o} S_o}} \quad (4).$$

The simulator XRD spectrum shown in Figure IV was used to explore this effect further. In this case, the peak falling at 44.5° was used to estimate the S/N ratio as a function of aperture area. In the shoulder at large Θ $CN_T = 41.6$. Equation 3 was then inverted to obtain $CN_{Xo} = 35.6$ when $CN_E = 2.7$. The simulator spectrum of Figure IV was acquired with $A_o = 130$ mm^2, and the intensity of the peak at 44.5° was measured to be 333 counts. Therefore, for this case, Equation 4 becomes

$$S/N = \frac{\frac{A}{130} 333}{\sqrt{(2.7)^2 + \left(\frac{A}{130} 35.6 + \sqrt{\frac{A}{130}} 35.6\right)^2 + \frac{A}{130} 333}} \quad (5).$$

This is plotted in Figure V which dramatically shows the effect of quantum fluctuations. Another way to appreciate the influence of the quantum effect is to imagine a system with *only* quantum noise. In this case, the signal-to-noise would be simply S/N = signal/noise = signal/(signal)$^{1/2}$ = (signal)$^{1/2}$ which is, in fact, the general functional behavior exhibited by the curve in Figure V.

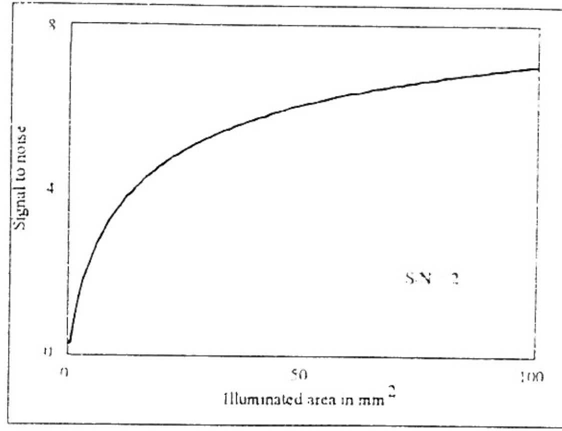

Fig. V. Calculated signal-to-noise versus aperture for the simulator XRD peak at 44.5° in Figure IV.

We might also ask what illumination area is necessary to achieve a specified signal-to-noise. When Equation 4 is inverted to express A as a function of S/N, the result is a quartic equation that can be solved numerically. For S/N = 2, generally considered the limit of resolution, A = 3.48 mm^2, which corresponds to a square with sides equal to 1.87 mm.

The foregoing discussion shows how the area of illumination affects the signal-to-noise of a XRD spectrum. Details will depend on the specific spectrometer, but these calculations suggest that XRD mapping of the surface may be a feasible in situ analysis tool for thin film deposition.

6.2. *Spatial Resolution Of the XRF Spectrum*

The methods used to estimate the spatial resolution of the XRD spectrum can be used to estimate the spatial resolution of the XRF system. A x-ray fluorescence spectrum consists of spectral lines whose intensities – once corrected for relative fluorescing strength – are proportional to the relative number of fluorescing species (Wachtman, 1993). The principal use of the XRF spectrum is the estimation of film stoichiometry, and this is equal to the ratio of the corrected intensities.

If the corrected intensities of two fluorescent lines are S_1 and S_2, then the stoichiometry may be defined as $x = S_1/S_2$. Associated with each of the two spectral lines is noise. Noise resulting from spurious scattering of x-rays can be greatly reduced by careful mechanical design. First, since fluorescent x-rays are radiated isotropically from the substrate, the detector can be positioned to minimize interception of scattered x-rays. Second, those that do reach the detector will have a spectral line characteristic of the x-ray source anode and can, therefore, be eliminated in many cases by simple signal processing. The

electronic noise can be ignored as it was for XRD. The noise voltages that cannot be eliminated so simply are $\sqrt{S_1}$ and $\sqrt{S_2}$. These sources are not correlated so that the uncertainty associated with a stoichiometry measurement is

$$CN_T = [(\sqrt{S_1})^2 + (\sqrt{S_2})^2]^{1/2} = [S_1 + S_2]^{1/2} \qquad (6).$$

This can be compared with Equation 4, the counting noise associated with a XRD measurement.

The XRF component of the in situ x-ray sensor system is still under development so that it is not possible at this time to estimate the XRF spatial resolution. That resolution will depend on the specific detector, substrate-to-detector distance, and divergent slit dimensions.

7. DATA ACQUISITION TIMES

Having estimated the effect of the aperture on spatial resolution for XRD, and the effect of noise on both the XRD and XRF spectrum, it is possible to estimate data acquisition times. The above analysis clearly demonstrates that unless the noise is dominated by the system electronic noise, increasing the counting time will not increase the signal-to-noise ratio. As discussed in Section 6, the electronic noise corresponds to a counting error of ± 2.7 so that by the time 100 counts have been accumulated, for example, system electronic noise will be insignificant and lengthening the counting time will not improve the signal-to-noise.

The simulator XRD spectrum of the WS_2 film in Figure IV serves as an example. The peak at 44.5° is 333 counts, well above the system electronic noise. The area of illumination used to acquire the spectrum shown in Figure IV was 130 mm^2, and the spectrum was obtained by counting at each point for 2 s. Assuming that N counts would sufficiently exceed the system electronic noise, and the area of illumination is A, the counting time at each angular position would be

$$t = \left(\frac{N}{333}\right)\left(\frac{130}{A}\right)2 \qquad (7)$$

The first term gives the change in time needed to acquire N counts. The second term gives the change in time needed to compensate for the aperture of area A. The last term is the counting time at each angular position used to acquire the spectrum of Figure IV. Suppose N = 100, i.e. N>>2.7,. and that a signal-to-noise of 4:1 is sufficient to analyze the XRD spectrum with the desired accuracy. Inversion of Equation 4, as before, gives an illumination area of A = 13.27 mm^2 or a square with 3.64 mm on a side. Using these values in Equation 7, t = 5.88 s per angular position.

If, as discussed above, useful information might be obtained by scanning a spectrum like that of Figure IV only from 33 - 50°, and if counts are accumulated only at 0.5° intervals for a total of 34 angular steps, then that portion of the spectrum could be obtained in 34 × 5.88 = 200 s with a signal-to noise of 4:1. It may be sufficient to record the intensity or position of only one peak. In that case, 5 angular positions may be enough to define the peak, and this would reduce data acquisition time to 5 × 5.88 = 29.4 s. This is only an example based on one XRD spectrum, but it does clearly indicate that it is necessary to plan the scanning procedure in advance.

8. XRD & XRF MAPPING

All the foundations needed to address this issue have been established in the preceding sections of this paper. Specifically, in Section 5 it was shown that the signal-to-noise associated with a XRD spectrum acquired with a square illumination area with 1.87 mm on a side would, under the conditions of the example, be 2:1, and for a 13.27 mm^2 illumination area, 3.64 mm on a side, would be 4:1 and would require 200 s to acquire a 34-point spectrum. Assuming that three points on the film are sufficient to determine film uniformity, it would require about 10 minutes to acquire the two significant XRD peaks in a spectrum like that for WS_2 shown in Figure IV.

Data acquisition time for a XRF spectrum is yet to be determined, and some innovative design concepts for XRF data acquisition are still under development. Yet even at this stage, it appears that the time required for acquisition of XRF spectra will be considerably less than required for acquisition of XRD spectra.

For either XRD or XRF, rastering the x-ray beam across a fixed substrate and film is not practical with the current AFRL design; the x-ray tube and detector must be very carefully aligned inside the sputtering chamber. However, the substrate stage in the AFRL system has both rotational *and* translations degrees of freedom. Thus, the surface of the film could be interrogated by moving the film relative to the x-ray beam.

8.1. Mapping film microstructural properties

When Omni Instruments' software program TXRDwin® is applied to each XRD spectrum, the program deconvolves overlapping spectral peaks and returns numerical values for all spectral parameters that are normally used in conjunction with international databases of XRD spectra to aid in identifying the species and crystal structure. These parameters include: peak locations, intensities, integrated areas, and line shape functions. Essentially, this is a table of parameter values with which the XRD spectrum could be reconstructed.

This set of numbers then can be used to determine microscopic film characteristics, as mentioned in Section 2., such as residual stress and crystal phase concentration.

For example, residual stress can be determined by comparing the locations of the XRD spectral peaks of the sputtered film with those of a standard film. These shifts are due to lattice strain from which stress in the film can be calculated using Stoney's equation (Stoney, 1909).

Relative crystal phase concentration can be determined by comparing the relative peak intensities of the XRD spectrum of the sputtered film with those produced by a standard film sample.

It is clear, therefore, that these film properties can be determined from XRD measurements only by comparing each XRD spectrum with a "standard" spectrum. It follows that it is essential that such a database be constructed in order to interpret correctly the in situ XRD spectra. This is especially true in light of the discussion regarding Figure IV which shows how the spectra obtained from in situ measurements in the AFRL sputtering chamber can differ from those obtained by conventional means. Thus, both an in situ and an ex situ database are needed to facilitate interpretation. Once interpretation is completed, the results can be presented on a multidimensional map, or used directly for process control.

8.2. *Mapping film stoichiometry*

It is considerably easier to develop maps related to XRF spectra. Although the type of detector that will be used with the AFRL x-ray system has not been finalized, it probably will be of the energy dispersive type (EDX). This detector, which may be thought of as a photomultiplier with a scintillating crystal, produces electrons whose energy is proportional to the incident x-ray energy, and whose electron density is proportional to the x-ray flux. The electron energy and density is measured by a charge sensitive amplifier whose output is presented to a multichannel pulse height analyzer (MPA). The analyzer output displays the distribution of energies. The relative intensities produced by the different fluorescing species is proportional to the relative density of those species within the x-ray area and volume illuminated. The position of the each peak in the spectrum is a function only of the fluorescing atom and is independent of the crystal structure. Thus, no complex interpretation is necessary. Film stoichiometry is simply computed from the normalized peak intensities. These normalized intensities then could be plotted on a multidimensional map with a different plane for each concentration.

From these XRD and XRF maps, it would be possible to determine the uniformity of crystal phase, residual stress, or stoichiometry. For example, nonuniformities could be due to the fact that the flux of the depositing species originating from the magnetron target, or the applied bias voltage was not uniform over the film. The deposition protocol could be modified by translating the substrate, possibly at a variable speed, beneath the magnetron, changing the bias, etc..

9. CONCLUSION

Ex situ x-rays provide an abundance of film properties information. The first goal of this effort has been to determine whether similar information can be acquired in situ and in near real time in the magnetron sputtering chamber. The second goal has been to determine whether materials properties maps can also be constructed in situ and in near real time, and whether these maps can be used to enhance film uniformity. A XRF map of the film surface is relatively easy to acquire. A XRD map is more difficult to produce. Nevertheless, information such as crystal phase concentration, texture, and residual stress is of such importance for thin film development that the effort is warranted, and will advance the state of the art in process control and image mapping.

This work, including the design, development, fabrication, and installation of the in situ x-ray sensor system for magnetron sputtering, is supported by the U. S. Air Force Research Laboratory under contract F33615-99-C-5702.

REFERENCES

Chapman, B. (1980). *Glow Discharge Processes – Sputtering and Plasma Etching*, John Wiley & Sons, New York.

Guinier, A.(1963). *X-ray Diffraction in Crystals, Imperfect Crystals, and Amorphous Bodies*, W. H. Freeman, San Francisco.

Robinson, F. N. H.(1963). *Noise In Electrical Circuits*, Oxford University Press, London.

Rossnagel, S. M.(1989). Magnetron Plasma Deposition Process. In: *Handbook of Plasma Processing Technology* (Rossnagel, S. M., *et al* (Eds)), Chapter 6. Noyes, New Jersey.

Stoney, G. G. (1909). *Proc. Roy. Soc.* Ser A82 172.

Thornton, J. A. (1974). *J. Vac. Sci. Technol.* **11**, 666.

Warren, B. E. (1969). *X-ray Diffraction*, Addison-Wesley, Redding, MA.

Wachtman, J. B. (1993). *Characterization of Materials*, Chapter 19, Butterworth-Heinemann, Boston.

Windishmann, H. (1992). Intrinsic Stress in Sputter-deposited Thin Films. In: *Critical Reviews in Solid State and Material Sciences*, **17**, 547.